NASA TECHNICAL NOTE

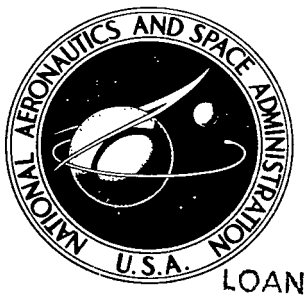

NASA TN D-4684

FISSION NEUTRON ATTENUATION IN LITHIUM-6, NATURAL LITHIUM HYDRIDE, AND TUNGSTEN

by Gerald P. Lahti

Lewis Research Center
Cleveland, Ohio

NATIONAL AERONAUTICS AND SPACE ADMINISTRATION • WASHINGTON, D. C. • AUGUST 1968

NASA TN D-4684

FISSION NEUTRON ATTENUATION IN LITHIUM-6, NATURAL LITHIUM HYDRIDE, AND TUNGSTEN

By Gerald P. Lahti

Lewis Research Center
Cleveland, Ohio

NATIONAL AERONAUTICS AND SPACE ADMINISTRATION

For sale by the Clearinghouse for Federal Scientific and Technical Information
Springfield, Virginia 22151 – CFSTI price $3.00

ABSTRACT

A fission-spectrum neutron-dose-rate-attenuation curve was computed by the discrete-ordinates method for Li^6H and natural LiH for penetration depths up to 139.5 cm. Results were compared with a recent Monte Carlo calculation for natural LiH. A single value for an energy-independent-neutron-removal cross section for Li^6 and natural Li in LiH was deduced for use in an Albert-Welton dose-attenuation kernel but is accurate for only a given range of penetration. The validity of fast-neutron-removal theory was demonstrated for the cases of W followed by LiH. From this penetration data, a neutron-removal cross section for W was calculated.

FISSION NEUTRON ATTENUATION IN LITHIUM-6, NATURAL LITHIUM HYDRIDE, AND TUNGSTEN

by Gerald P. Lahti

Lewis Research Center

SUMMARY

The calculated attenuation of dose due to a point source of uranium-235 fission-spectrum neutrons through lithium-6 hydride (Li^6H) is presented. The computations were made with the use of a one-dimensional discrete-ordinates transport code. The single-scatter rad dose was calculated to a depth of 139.5 centimeters. A similar calculation was performed for natural lithium hydride (LiH) and compared with recently published Monte Carlo results for the same configuration. The results are within 25 percent of the smoothed Monte Carlo results at deep penetration depths. Li^6H and LiH offer similar attenuation properties; because of its 12-percent lower density, Li^6H offers a reduction in weight over LiH.

An attempt was made to deduce a single energy-independent neutron-removal cross section for Li^6 and Li in LiH for use in an Albert-Welton dose-attenuation kernel utilized by point-kernel shielding codes. Although no single value gave close agreement to the calculated results over the entire range, values of 0.100 and 0.115 square centimeter per gram for natural Li and Li^6, respectively, in LiH gave the best agreement. A better fit of the dose attenuation is afforded by a dose-attenuation kernel for LiH of the form $a_0 \exp(a_1 r + a_2 r^2 + a_3 r^3)$, where the a's are constants and r is the distance from the source.

The validity of the fast-neutron-removal theory for cases of tungsten (W) followed by Li^6H or LiH is demonstrated for cases of a point-fission source surrounded by up to 25.5 centimeters of W followed by Li^6H or LiH. A fast-neutron-removal cross section of 0.0105 ± 0.001 square centimeter per gram for W provides a good fit to the calculated data.

INTRODUCTION

Lithium-6 hydride (Li^6H) is a neutron shield material of interest because the use of

the lithium-6 isotope with its high (n,α) cross section results in the depression of secondary gammas (arising from (n,γ) events) in shields involving both neutron and gamma shield arrangements. Also, Li^6H has a lower density than that of natural lithium hydride (LiH), so that it offers the additional possibility of reduction in shield weight, provided that it is as good a fast-neutron (dose) attenuator as LiH.

A series of discrete-ordinates calculations was made to compare the fast-neutron-dose attenuation of LiH and Li^6H and to generate removal cross sections for use in point-kernel shielding codes (e.g., QAD, refs. 1 and 2). The calculations were made with the use of the one-dimensional discrete-ordinates transport code ANISN (ref. 3) for a small (point) source emitting a fission spectrum of neutrons in an essentially infinite medium of LiH and Li^6H. A comparison was made between the discrete-ordinates calculation for LiH and a recent Monte Carlo calculation (ref. 4) made for the same configuration. Similar calculations were made for the cases of tungsten (W) followed by Li^6H or LiH to demonstrate the validity of fast-neutron-removal theory and to obtain a fast-neutron-removal cross section for W.

FISSION NEUTRON ATTENUATION IN LITHIUM-6 HYDRIDE AND LITHIUM HYDRIDE

Details of Input to Calculations

The discrete-ordinates code ANISN was used to make transport calculations for the cases of a uranium-235 (U^{235}) fission-spectrum source located at the center of a 139.5-centimeter-radius sphere of LiH or Li^6H. The computations were made with the use of multigroup cross sections generated by GAM II (ref. 5) for the 25 fast energy groups indicated in table I.

The energy group structure is designed to place emphasis on that energy region contributing most to the neutron dose. A more detailed discussion of the energy group structure may be found in the section, Importance of Fine Group Structure Above 6 MeV. A single thermal group cross section was added to complete the considered energy span from 14.9 to 0.0 MeV. A 16-point full-range Gauss-Legendre quadrature scheme was used to describe the angular fluxes. The P_3 approximation was used to describe the elastic-scatter-source term. The mesh spacing used is indicated in table II.

The U^{235} fission-spectrum source (ref. 5) was assumed to be spread over the first five mesh intervals to facilitate the computation. The flux-to-dose conversion factors used were taken from figure 1 of reference 6 and are listed in table I. The resulting dose is a first-collision-rad dose. The density of natural LiH used was 0.75 gram per

TABLE I. - ENERGY GROUP STRUCTURE AND FLUX-TO-DOSE CONVERSION FACTORS

Group	Lower energy limit of group, E, eV	Flux-to-dose conversion factor, $4\pi r^2 \times$ Dose, (rad/hr)/(neutron/(cm^2)(sec))
1	13.5×10^{6}	2.05×10^{-5}
2	12.2	2.05
3	11.1	2.05
4	10.0	2.05
5	9.0	2.05
6	8.2	2.05
7	7.4	1.84
8	6.7	1.84
9	6.1	1.84
10	5.5	1.76
11	5.0	1.69
12	4.5	1.66
13	4.1	1.62
14	3.7	1.62
15	3.0	1.55
16	2.5	1.37
17	2.2	1.15
18	1.8	1.12
19	1.35	1.08
20	1.10	.935
21	.91	.83
22	.55	.72
23	.11	.54
24	3.0×10^{3}	.072
25	$.4\times10^{0}$	.0036
26	0	.004

TABLE II. - MESH SPACING FOR DISCRETE-ORDINATES PROBLEM

Range of penetration depth, r, cm	Mesh interval size, cm
0 to 6.0	0.4
6.0 to 10.5	.75
10.5 to 139.5	1.00

TABLE III. - DENSITIES OF LITHIUM-6, LITHIUM-7, AND HYDROGEN USED IN LITHIUM HYDRIDE CALCULATIONS

Constituent isotopes in -	Density, ρ	
	g/cm^3	$atoms/cm^3$
Natural lithium hydride:		
Hydrogen	0.0951	0.056837×10^{24}
Lithium-6	.0421	.004217
Lithium-7	.6130	.052619
Total	0.750	----------
Lithium-6 hydride:		
Hydrogen	0.0951	0.056837×10^{24}
Lithium-6	.5677	.056837
Total	0.6628	----------

cubic centimeter. The density of each of the constituent isotopes making up LiH and Li^6H is listed in table III. The density of Li^6H was calculated to be 0.6628 gram per cubic centimeter. The hydrogen atom density in Li^6H was assumed to be unchanged from that in the natural LiH, and the Li^7 atom was assumed to be replaced by Li^6.

Results of Discrete-Ordinate Calculations for Lithium Hydride

Comparison of attenuation properties of lithium hydride and lithium-6 hydride. - Semilogarithmic plots of the attenuation of neutron dose in LiH and Li^6H are shown in figure 1. The expression $4\pi r^2 \times$ Dose $((cm^2)(rad/hr)/(fission\ neutron/sec))$ is plotted against r, the distance from the center of the source. (All symbols are defined in appendix A.)

The dose in Li^6H is about 10 percent below that of LiH for r of about 30 centimeters, is about the same at 65 centimeters, and is about 60 percent above that of LiH at a depth of 120 centimeters. Small differences in neutron attenuation by Li^6H and LiH have been reported for experiments performed with 4- and 12-inch (10.16- and 30.48-cm) (ref. 7) and 36-inch (91.44-cm) (ref. 8) slabs of LiH and Li^6H. Both curves in figure 1 are concave upward after a penetration of about 30 centimeters, which indicates a con-

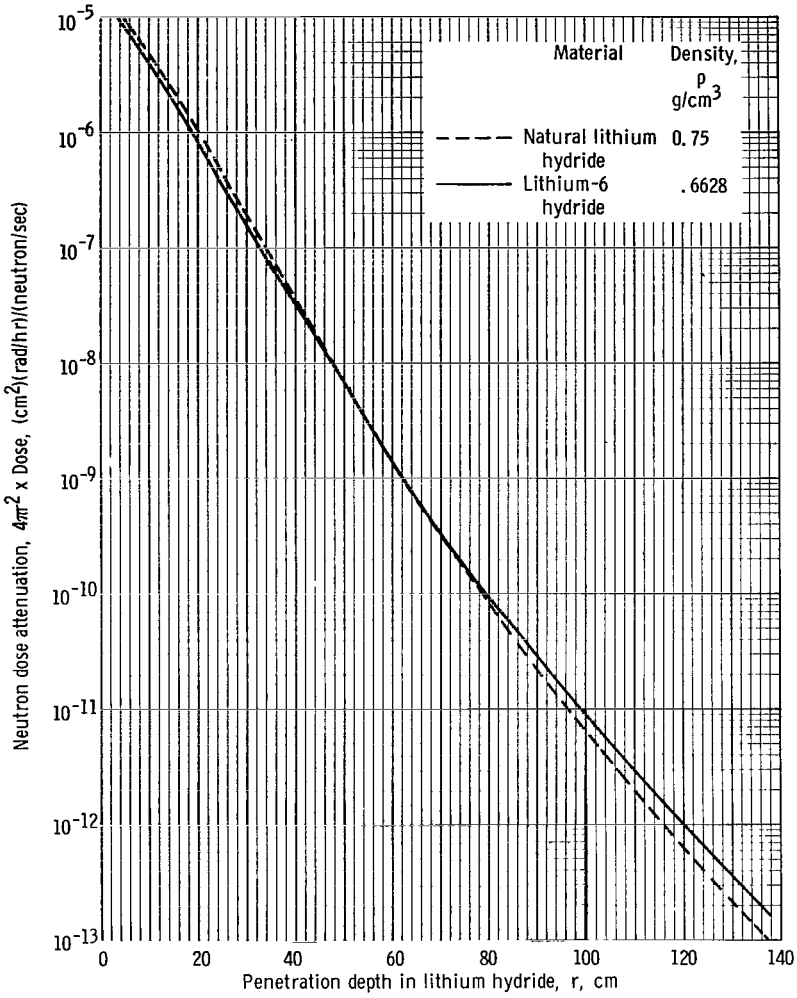

Figure 1. - Neutron dose attenuation in lithium hydride as calculated by discrete-ordinates method.

tinually hardening spectrum. Table IV lists the local attenuation coefficient μ where the dose attenuation of figure 1 is assumed to be of the form $Ar^{-2} \exp(-\mu r)$, or in terms of the density ρ and the mass thickness ρr, $Ar^{-2} \exp\left[-(\mu/\rho)(\rho r)\right]$, where A is a constant. The local attenuation coefficient decreases with increasing depth in LiH. At a depth of 130 centimeters, each curve of figure 1 appears to attain a constant slope defined by a single exponential. The value of this slope, as indicated in table IV, is 0.112 per centimeter (0.168 cm^2/g) for Li^6H and 0.1115 per centimeter (0.149 cm^2/g) for LiH.

Shielding effectiveness of lithium-6 hydride and lithium hydride. - With respect to fast-neutron-dose attenuation, Li^6H is favored over LiH because of the slight weight advantage it offers. For example, both afford the same attenuation at a 60-centimeter

TABLE IV. - VALUES OF LOCAL DOSE-ATTENUATION COEFFICIENTS

Penetration depth, r, cm	Local dose-attenuation coefficient			
	μ, cm^{-1}		μ/ρ, cm^2/g	
	Lithium-6 hydride	Lithium hydride	Lithium-6 hydride	Lithium hydride
30	0.1639	0.166	0.247	0.221
40	.1602	.165	.242	.220
50	.1556	.160	.235	.213
60	.144	.152	.217	.203
70	.136	.144	.205	.192
80	.127	.136	.191	.181
90	.119	.128	.179	.171
100	.113	.122	.171	.163
110	.113	.115	.171	.153
120	.113	.1115	.171	.149
130	.112	.1115	.168	.149

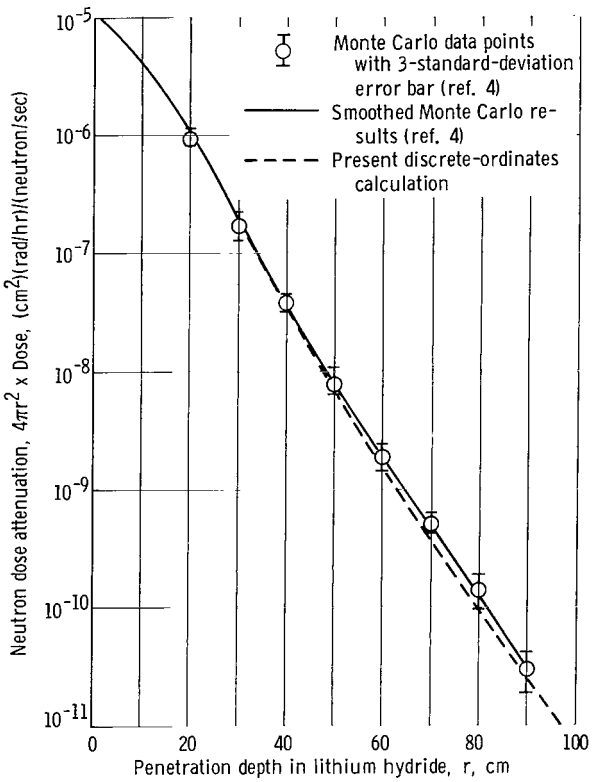

Figure 2. - Neutron dose attenuation in lithium hydride as calculated by Monte Carlo method. Lithium hydride density, 0.75 gram per cubic centimeter.

depth, but Li^6H is 88 percent as dense as LiH (a 12-percent weight reduction). However, the weight advantage may decrease at deep penetration depths.

Comparison of discrete-ordinate results with Monte Carlo results. - Shown in figure 2 is a semilogarithmic plot of the expression $4\pi r^2 \times$ Dose $((cm^2)(rad/hr)/$ (fission neutron/sec)) against r for LiH as calculated by ANISN. Also included are the Monte Carlo results of Kam and Clark (ref. 4) shown with 3-standard-deviation error bars and a smoothed curve of the Monte Carlo results. The discrete-ordinates results are virtually the same as the smoothed Monte Carlo results to a depth of 40 centimeters. For deeper penetrations, the present calculations are lower than the smoothed Monte Carlo results by, at most, 25 percent.

A calculation was made to ascertain the effect of the approximation to the elastic-scatter-source term on the discrete-ordinate-calculation results. The P_1 approximation result (for both Li^6H and LiH) is 10 percent below the P_3 result at 40 centimeters ($2\frac{1}{2}$ decades of attenuation) and 50 percent lower at 120 centimerers (about $7\frac{1}{2}$ decades of attenuation). To obtain accurate results at deep penetration depths requires the P_3 scattering approximation; at shallow penetrations, P_1 scattering is adequate.

Another possible source of discrepancy in these results is due to the choice of the multigroup structure, which is discussed in more detail in the section Importance of Fine Group Structure Above 6 MeV.

Curve Fits to Discrete Ordinates Results

Evaluation of lithium removal cross section. - A dose kernel that is often used in point-kernel shielding codes to estimate the fast-neutron dose is the Albert-Welton kernel, which is of the form

$$4\pi r^2 D = \alpha_1 \, e^{-c} \, h^{\alpha_2} \, \exp(-\alpha_3 h^{\alpha_4})$$

where

D	dose rate from a unit source of fission-spectrum neutrons at a distance r
$\alpha_1, \alpha_2, \alpha_3, \alpha_4$	coefficients used to account for attenuation in hydrogen
c	$\sum_M \left(\frac{\Sigma_R}{\rho}\right)_M (\rho t)_M$

e^{-c} removal term accounting for attenuation due to all nonhydrogenous material

h equivalent thickness of hydrogen with density of 0.111 g/cm^3 encountered between source and receiver point

$\left(\frac{\Sigma_R}{\rho}\right)_M$ fast-removal cross section for M^{th} element

$(\rho t)_M$ mass thickness of M^{th} element

One set of coefficients α that describe neutron penetration in hydrogen are

$$\alpha_1 = 8.35\times10^{-5} \quad ((cm^2)(rad/hr)/(neutron/sec))$$

$$\alpha_2 = 0.29 \quad \text{(dimensionless)}$$

$$\alpha_3 = 0.83 \quad \text{(dimensionless)}$$

$$\alpha_4 = 0.58 \quad \text{(dimensionless)}$$

A value of Σ_R/ρ for lithium is deduced for use in the Albert-Welton kernel by assuming the framework of this kernel to be valid for LiH with Σ_R/ρ as the only adjustable parameter. (Refs. 7 and 8 have also estimated the value of Σ_R/ρ for Li in LiH with the use of Albert-Welton kernel as a framework for a curve fit.) Figure 3 is plot of Albert-Welton kernel evaluations for several values of Σ_R/ρ. Also shown for reference is the appropriate P_3 discrete-ordinates result. Figure 3(a) illustrates Albert-Welton kernel evaluations for values of Σ_R/ρ = 0.0876 (refs. 9 and 10), 0.100 (ref. 7), and 0.107 (ref. 8) square centimeter per gram for LiH[1]. The value of 0.100 square centimeter per gram provides the best fit to the discrete-ordinates results for natural LiH. For the matching of the Li^6H P_3 calculation (fig. 3(b)), a value of Σ_R/ρ = 0.115 square centimeter per gram fits well from penetration depths of 40 to 90 centimeters. Accurate fits are obtained in either LiH or Li^6H over a limited range of penetrations.

---

[1]The Σ_R/ρ of refs. 9 and 10 is a slab-removal cross section determined in early Lid-Tank experiments. Also, the value of Σ_R/ρ of 0.100 cm^2/g was deduced from ref. 7 with the assumption that a density of 0.75 g/cm^3 for LiH (Li density is 0.655 g/cm^3) is to be used with the reported value of Σ_R = 0.0655 cm^{-1}. Similarly, ref. 8 indicates a $\Sigma_R \cong 0.07$ cm^{-1} for Li in LiH with a density of 5.64×10^{22} atoms/cm^3.

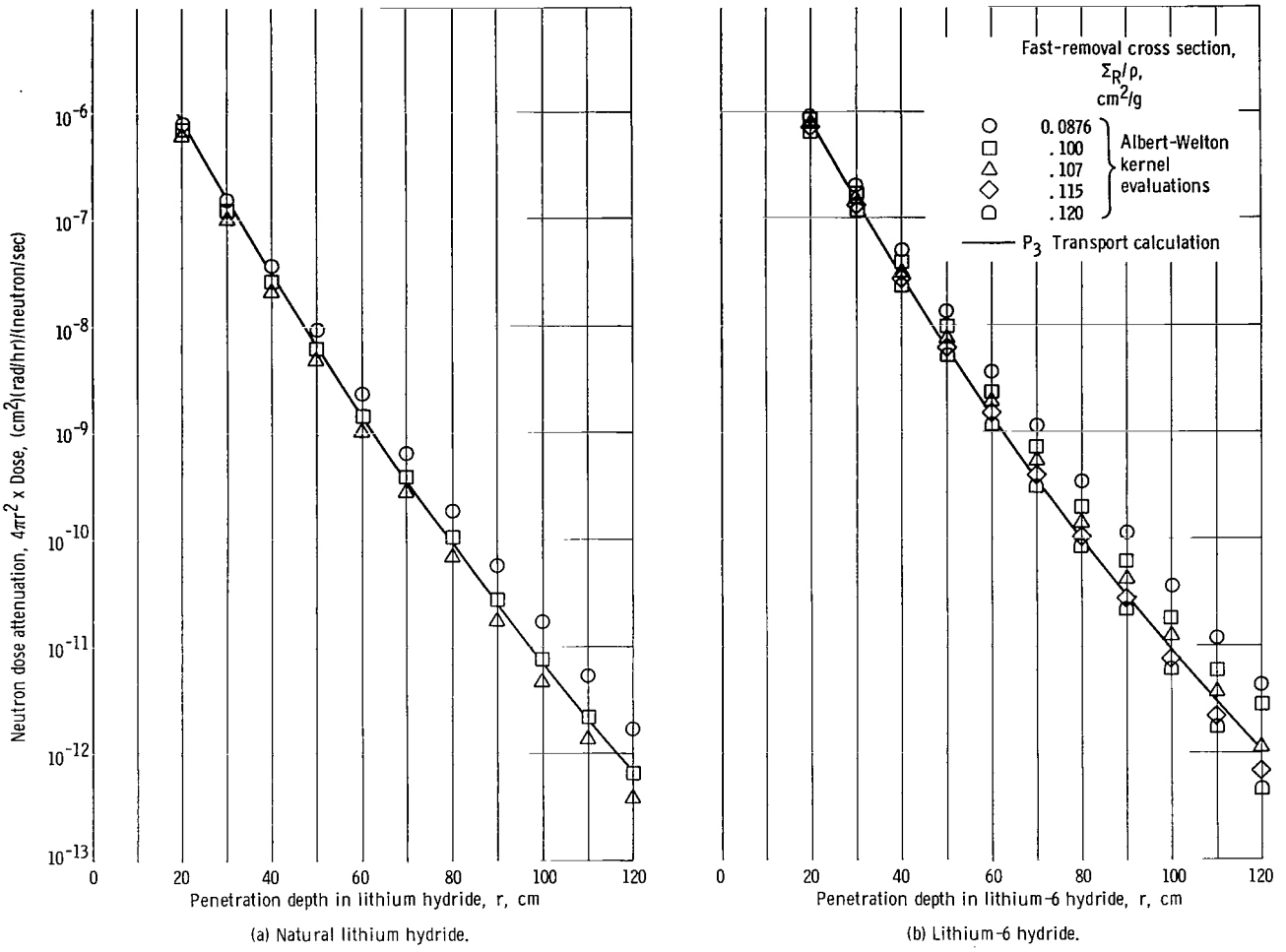

(a) Natural lithium hydride.

(b) Lithium-6 hydride.

Figure 3. - Curve fits for neutron attenuation in lithium hydride.

TABLE V. - COEFFICIENTS FOR LITHIUM HYDRIDE

DOSE KERNEL (EQ. (1))

Coefficient	Lithium hydride	Lithium-6 hydride
a_0	4.1595×10^{-5}	3.6550×10^{-5}
a_1	-1.8923×10^{-1}	-1.9597×10^{-1}
a_2	3.2378×10^{-4}	5.1652×10^{-4}
a_3	3.8022×10^{-8}	-7.8209×10^{-7}

Alternate fit to lithium hydride attenuation curve. - As shown in figure 3, the Albert-Welton kernel does not fit either the magnitude or the slope of the calculated dose curve over the entire interval. A better fit to the curve of LiH attenuation for both magnitude and slope is offered by a function of the form

$$4\pi r^2 \times \text{Dose} = a_0 \exp(a_1 r + a_2 r^2 + a_3 r^3) \tag{1}$$

where r is the depth (cm) of LiH. Coefficients for LiH and Li^6H were calculated by use of a least-squares fit to the data curves of figure 1 and are listed in table V.

Equation (1), with the appropriate coefficients, obtains values of $4\pi r^2 \times$ Dose which are within ±5 percent of the values calculated with the transport code over the range of r from 20 to 139.5 centimeters (fig. 1). An attenuation kernel of the form of equation (1) could be employed in a point-kernel code for layered configurations of high Z-layers with LiH. The addition of a removal term e^{-c} as described previously for the Albert-Welton kernel, is required to account for fast-neutron attenuation in high Z-layers.

FISSION NEUTRON ATTENUATION IN TUNGSTEN AND LITHIUM HYDRIDE

The neutron-removal theory used in neutron shielding calculations may be stated as the following equation for the case of a point source of fission-spectrum neutrons surrounded by a high Z- (atomic number) material followed by a hydrogenous material:

$$4\pi r_1^2 \times \text{Dose}\,(t_Z, t_H) = 4\pi r_2^2 \times \text{Dose}\,(0, t_H) \exp\left(-\frac{\Sigma_R}{\rho}\right)_Z (\rho t)_Z \tag{2}$$

where

$r_1 = t_H + t_Z$

Dose (t_Z, t_H) dose observed at distance r_1 from point source with t_Z cm of high Z-material followed by t_H cm of hydrogenous material surrounding the source

t_Z thickness of high Z-material, cm

t_H thickness of hydrogenous material, cm

$r_2 = t_H$

TABLE VI. - ALTERNATE ENERGY GROUP STRUCTURE

AND FLUX-TO-DOSE CONVERSION FACTORS

Group	Upper energy limit of group, E, eV	Flux-to-dose conversion factor, $4\pi r^2 \times$ Dose, (rad/hr)/(neutron/(cm^2)(sec))
1	14.92×10^{6}	2.05×10^{-5}
2	12.21	2.05
3	10.00	2.05
4	8.19	1.84
5	6.07	1.76
6	4.97	1.66
7	4.07	1.51
8	3.01	1.37
9	2.47	1.15
10	2.23	1.12
11	1.83	1.08
12	1.35	.94
13	1.11	.83
14	.91	.72
15	.55	.65
16	.41	.54
17	.11	.17
18	1.50×10^{4}	3.2×10^{-7}
19	3.35×10^{3}	7.2×10^{-8}
20	5.83×10^{2}	1.3×10^{-8}
21	1.01×10^{2}	3.6×10^{-9}
22	2.90×10^{1}	3.6×10^{-9}
23	1.07×10^{1}	5.4×10^{-9}
24	3.06×10^{0}	9.5×10^{-9}
25	1.13	1.5×10^{-8}
26	.41	4.0×10^{-8}

Dose $(0, t_H)$	dose observed at distance r_2 from point source with t_H cm of hydrogenous shield surrounding only the point source
$(\Sigma_R/\rho)_Z$	high Z-material-effective removal cross section, cm^2/g
ρ	density of high Z-material, g/cm^3
$(\rho t)_Z$	$= \rho \times t_Z$

This formulation simply separates the dose-attenuation kernel into two parts: one is due to the high Z-material, and the other is due to the hydrogenous material, which functions as if the high Z-component were not present. (Details of this formulation may be found in refs. 11 or 12.) This theory has been investigated by discrete-ordinates calculations for cases of several thicknesses (6, 10.5, 20.5, and 25.5 cm) of W at a density of 19.3 grams per cubic centimeter followed by Li^6H or LiH. In these calculations, the mesh spacing indicated in table II and the energy group structure of table VI were used. The energy group structure is revised from that of table I so that neutrons slowing down from the inelastic collisions with W might be followed more accurately. At deep penetrations, the difference in neutron dose resulting from the use of this choice of energy group structure instead of that of table I is less than 10 percent at a depth of 90 centimeters for the case of figure 1.

Results of Discrete-Ordinates Calculations for Tungsten and Lithium Hydride

Effective attenuation of fission neutrons by tungsten. - Figure 4 is a plot of $4\pi r^2 \times \text{Dose}\ ((cm^2)(rad/hr)/(\text{fission neutron/sec}))$ against the depth of penetration in the LiH following W, as obtained by the discrete-ordinates calculation. Figure 4(a) is for W thicknesses of 0, 6, 10.5, 15.5, 20.5, and 25.5 centimeters followed by Li^6H. Figure 4(b) is for W thicknesses of 0, 6, 10.5, and 15.5 centimeters-followed by natural LiH. If the removal theory formulation is valid, the resulting curves should be separated from the case of LiH without the presence of W by the constant factor $\exp\left[(\Sigma_R/\rho)_W(\rho t)_W\right]$ where $(\Sigma_R/\rho)_W$ is the removal cross section for W and $(\rho t)_W$ is the mass thickness of W. Inspection of figure 4 shows that an approximately constant factor separates the two curves after a LiH penetration of about 20 centimeters, a minimum penetration required to restore the spectrum to that characteristic of LiH. Table VII lists ratios of dose without W to dose with W (the apparent attenuation for a given thickness of W) for several depths in LiH as calculated by the discrete-ordinates code. Also included in the table is the effective removal cross section for W that is calculated from equation (2).

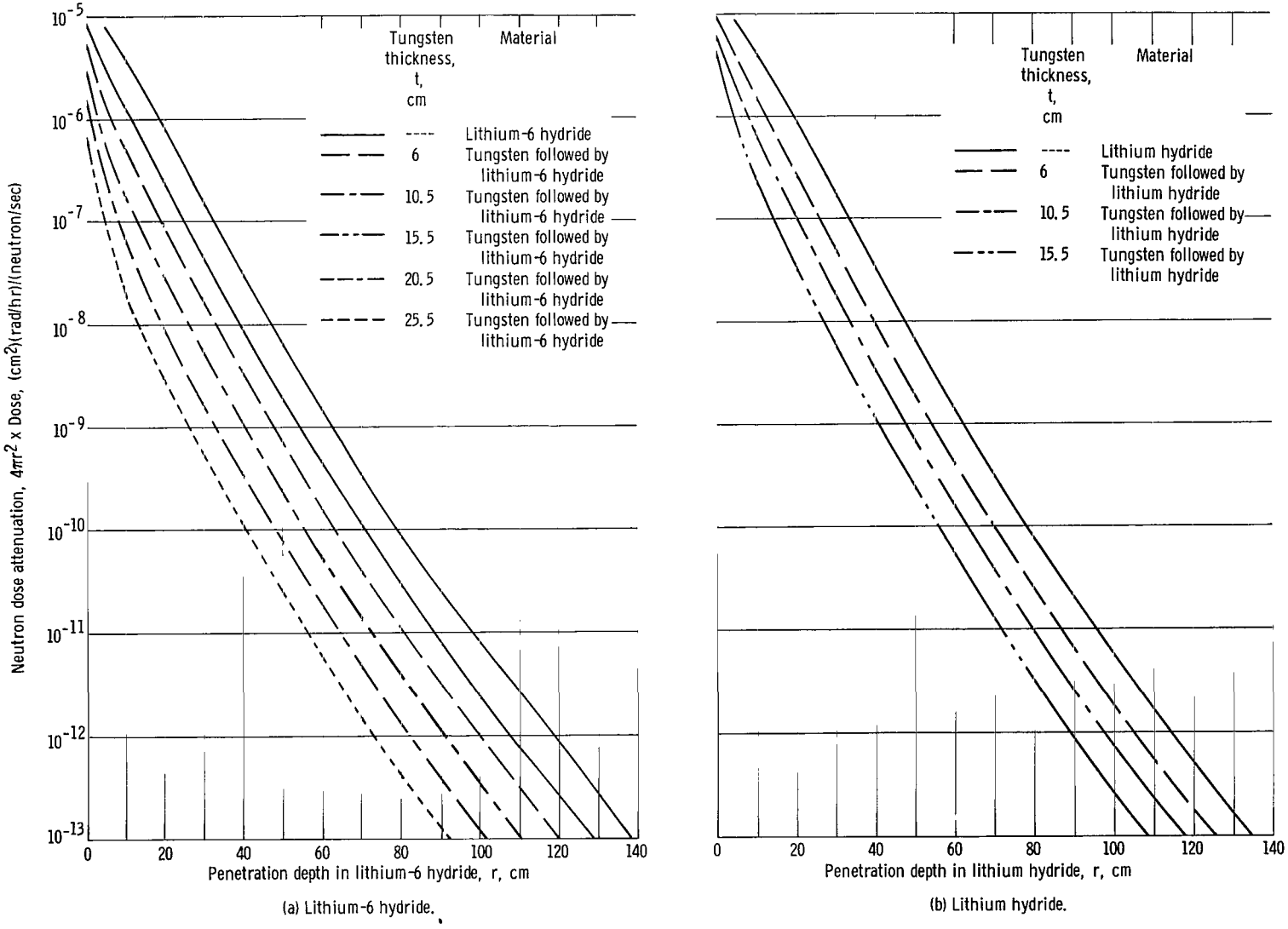

(a) Lithium-6 hydride.

(b) Lithium hydride.

Figure 4. - Discrete-ordinates calculation of fission neutrons in tungsten followed by lithium hydride.

TABLE VII. - APPARENT ATTENUATION AND EFFECTIVE REMOVAL CROSS SECTION FOR TUNGSTEN FOLLOWED BY LITHIUM HYDRIDE

Penetration depth, r, cm	Ratio of dose without tungsten to dose with tungsten,[a] $\frac{4\pi r^2 \times \text{Dose}(0, t_{LiH})}{4\pi r^2 \times \text{Dose}(t_W, t_{LiH})}$					Calculated effective removal cross section, Σ_R/ρ, cm^2/g				
	Thickness of tungsten, t_W, cm					Thickness of tungsten, t_W, cm				
	6	10.5	15.5	20.5	25.5	6	10.5	15.5	20.5	25.5
Lithium-6 hydride										
30	3.41	9.28	29.0	91.8	292	0.01060	0.01100	0.01126	0.01140	0.01153
40	3.41	9.24	28.5	89.0	280	.01060	.01096	.01120	.01134	.01145
50	3.35	8.91	27.0	82.7	254	.01045	.01080	.01102	.01115	.01125
60	3.28	8.59	25.4	76.2	231	.01025	.01058	.01082	.01095	.01106
70	3.30	8.19	23.8	66.6	197	.01030	.01036	.01060	.01075	.01086
80	3.16	7.93	22.85	64.2	189	.00993	.01022	.01046	.01060	.01073
90	3.09	7.76	22.15	62.8	186	.00973	.01012	.01035	.01050	.01065
100	3.07	7.64	21.7	62.3	---	.00968	.01003	.01029	.01045	.01062
110	3.05	7.58	21.5	----	---	.00960	.00999	.01025	.01043	------
Lithium hydride										
30	3.43	9.31	29.1	----	---	0.01062	0.01101	0.01126	-------	-------
40	3.42	9.30	28.9	----	---	.01058	.01100	.01124	-------	-------
60	3.24	8.55	25.8	----	---	.01015	.01060	.01086	-------	-------
80	3.06	7.85	22.8	----	---	.00966	.01017	.01045	-------	-------
100	2.94	7.42	21.2	----	---	.00931	.00990	.01020	-------	-------

[a]From fig. 4.

Effective removal cross section for tungsten. - From the foregoing remarks and the data of table VII, it may be concluded that simple removal theory will give reasonable results for deep penetration problems involving up to 25.5 centimeters of W and 110 centimeters of LiH for single W-layer configurations for depths in LiH greater than 30 centimeters. The calculated effective removal cross sections for W listed in table VII can be compared with the two experimentally observed values of 0.01145± 0.00065 and 0.01025±0.00082 square centimeter per gram and with the weighted average values of 0.0100 square centimeters per gram (given in ref. 10). All the values of calculated Σ_R/ρ for W fall within the experimental errors reported. An increase occurs in the effective removal cross section of W with W thickness and a decrease occurs with LiH thickness. The value of $\Sigma_R/\rho = 0.0105 \pm 0.001$ square centimeter per gram covers the entire range calculated.

Neutron spectra in tungsten and lithium hydride. - Another interesting result is illustrated in figure 5, a plot of the relative integral neutron spectrum (i.e., the fraction of neutron flux above some energy E)[2] for several values of E against the distance from the source r. The dashed curves are for the case of a point-fission source in Li^6H, and the solid curves are for the case of a point-fission source surrounded by 15.5 centimeters of W followed by 124 centimeters of Li^6H.

For the case of 15.5 centimeters of W followed by Li^6H, the neutron spectrum is shifted by nonelastic scattering events in W. The energy spectrum of neutrons leaking from the W (at r = 15.5 cm) is about 40 percent in the energy interval of 110 to 410 KeV and another 35 percent in the interval of 15 to 110 KeV, which is much different from the fission spectrum. After about 25 centimeters of penetration in Li^6H, the relative spectra (for the case of W followed by Li^6H) are virtually the same as for the case of Li^6H alone. (If the solid curve (W-Li^6H) were plotted against depth in Li^6H, it would be shifted 15.5 centimeters to the left, which would result in almost the same values that are plotted for the dashed (Li^6H only) curve after the spectrum has reached equilibrium.) Regardless of the low-energy-leakage spectrum, the high energy flux, greater than 6 or 8 MeV, leaking from the high Z-shield (or source) gives rise to the characteristic spectrum shape and magnitude at deep penetrations in hydrogenous materials. A tabulation of multigroup fluxes at various penetrations of LiH and Li^6H appears in appendix B.

Importance of Fine Group Structure Above 6 MeV

Figure 5 illustrates how the fraction of neutrons above 6 MeV (and the fraction of dose attributable to them) increases with penetration depth. At one point in this series of computations, an alternate, coarser 14-group structure was used to ascertain its effect on calculated dose. This structure had only one energy group in the region extending from 6.1 to 14.9 MeV, as compared with the 26-group set of table VI with four energy groups in the region. The dose in the 14-group result was lower than that for the 26-group set at the following depths in LiH: 10 percent at 40 centimeters, 45 percent at 70 centimeters, a factor of 2 at 90 centimeters, and a factor of 8.5 at 120 centimeters. The increasing error in the 14-group calculation is directly attributable to the lack of definition above 6 MeV; more precisely, the calculation lacks a correct description of neutron transport characteristics above 6 MeV, that is, neutrons whose energy spectrum changes greatly with the penetration depth and is no longer that calculated by the infinite-medium cross-section code (GAM-II) for a single group above 6 MeV. At a 120-centimeter penetration, each of the four groups above 6 MeV in the 26-group calculation

[2]This fraction is equal to $\int_E^\infty \varphi(r, E)\, dE \Big/ \int_0^\infty \varphi(r, E)\, dE$.

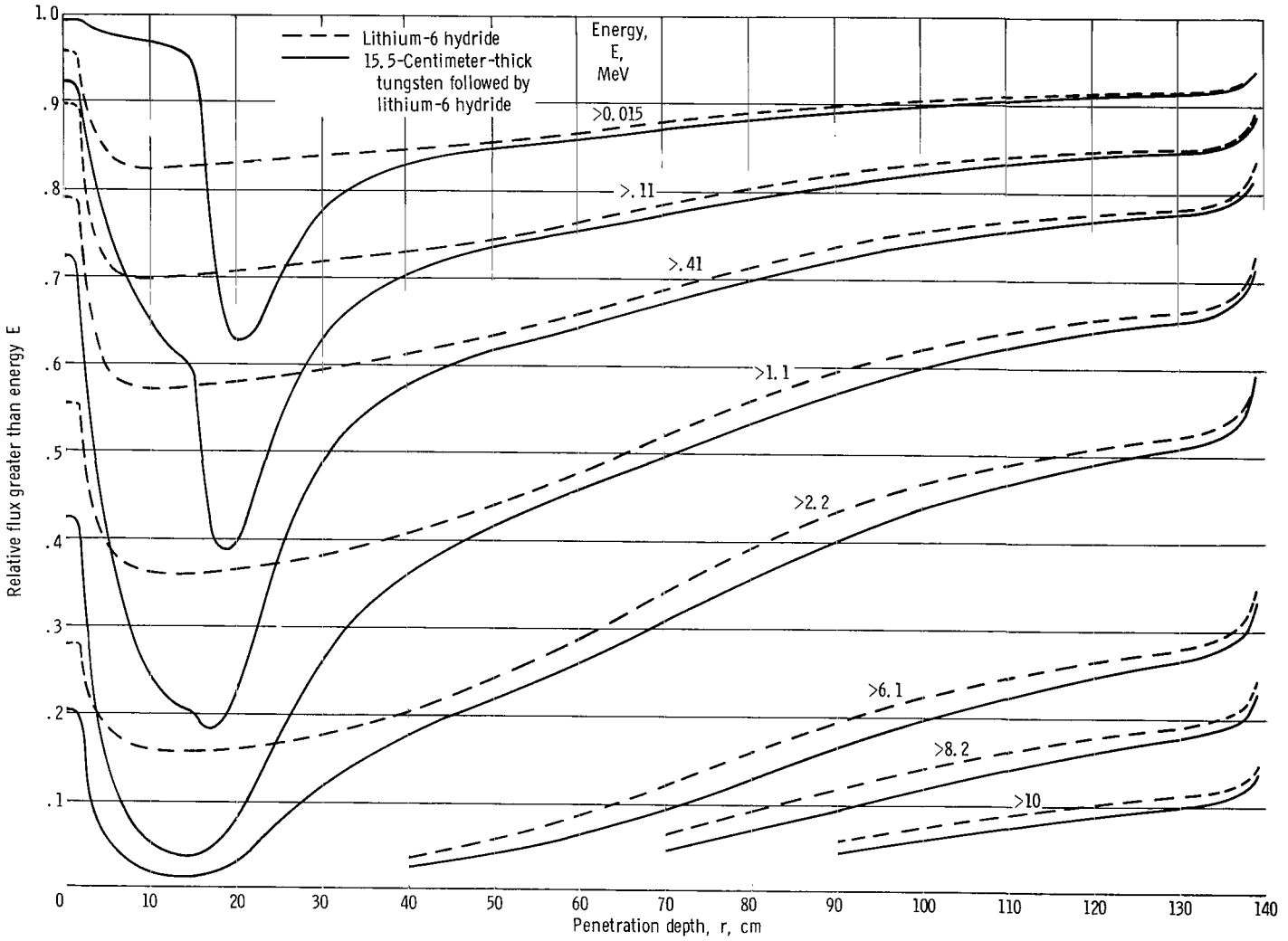

Figure 5. - Relative flux in tungsten and lithium-6 hydride.

contributes about 10 percent to the total dose. The average energy of those neutrons above 6 MeV (see fig. 5) shifts from 7.48 MeV, as calculated by GAM-II for the infinite medium, to 7.60 MeV at 20 centimeters, to about 8.5 MeV at 60 centimeters, and to 9.2 MeV at 100 centimeters.

CONCLUDING REMARKS

A fission-spectrum neutron-dose-rate-attenuation curve was computed by the discrete-ordinates method for lithium-6 hydride (Li^6H) and natural lithium hydride (LiH) at penetrations up to 139.5 centimeters for the case of a point source of fission-spectrum neutrons in an essentially infinite medium. Results were compared with a Monte Carlo calculation for natural LiH and were in general agreement. On the basic of penetration depth, Li^6H and LiH offer comparable attenuation properties.

If the Albert-Welton kernel for fast-neutron-dose attenuation is used for LiH or Li^6H at deep penetrations (10^6 to 10^8 attenuation), a value of 0.100 or 0.115 square centimeter per gram should be used for the fast-removal cross section of natural Li or Li^6, respectively, in LiH. These values result in an approximate fit to the discrete-ordinates results for a given range of attenuation. A better fit is offered by a single kernel for LiH of the form $a_0 \exp(a_1 r + a_2 r^2 + a_3 r^3)$.

The removal theory was demonstrated to describe the attenuation of fission-neutron dose for cases of a fission-spectrum source surrounded by tungsten followed by Li^6H or LiH after a penetration of about 30 centimeters in LiH. A good fit was provided by the description of the tungsten dose attenuation given by the exponential $\exp\left[-(\Sigma_R/\rho)(\rho t)\right]$ with $\Sigma_R/\rho = 0.0105 \pm 0.001$ square centimeter per gram. This fit is in agreement with experimental results.

Accurate discrete-ordinates results were obtained with P_1 scattering and a coarse group structure to a depth of 40 centimeters in LiH; for deeper penetration, P_3 scattering and a fine high-energy (greater than 6 MeV) group structure is required.

Lewis Research Center,
National Aeronautics and Space Administration,
Cleveland, Ohio, April 25, 1968,
124-09-01-03-22.

APPENDIX A

SYMBOLS

A	constant in dose-kernel expression
a_0, a_1, a_2, a_3	constants in alternate dose kernel
c	e^{-c} accounts for neutron attenuation in high Z-material
E	energy, MeV
h	equivalent hydrogen thickness, cm
r	radius (penetration depth or distance from center of source), cm
t	thickness, cm
Z	atomic number
$\alpha_1, \alpha_2, \alpha_3, \alpha_4$	constants in Albert-Welton dose kernel
μ	local dose-attenuation coefficient, cm^{-1}
μ/ρ	local mass dose-attenuation coefficient, cm^2/g
ρ	density, g/cm^3
ρt	mass thickness, g/cm^2
Σ_R	fast-neutron-removal cross section, cm^{-1}
Σ_R/ρ	mass fast-neutron-removal cross section, cm^2/g
φ	neutron flux, neutrons/(cm^2)(sec)

Subscripts (used with Σ_R/ρ, ρt, and t):

M	M^{th} element other than hydrogen
W	tungsten
Z	high-Z material

APPENDIX B

NEUTRON FLUX IN LITHIUM HYDRIDE

Of possible interest are the numerical values of the neutron flux as a function of the distance from the source for the case of a point source of fission neutrons (1 fission neutron/sec) in LiH, as calculated by the discrete-ordinates method. This appendix contains values of the multigroup fluxes for values of r of 15, 30, 60, 90, and 120 centimeters and for the group structure of table VI. The values given represent the multigroup fluxes

$$\int_{E_{i-1}}^{E_i} \varphi(E, r)\, dE \equiv \varphi_i(r)$$

The values of $\varphi_i(r)$ are listed in table VIII(a) for the case of a point source in LiH and in table VIII(b) for the case of a point source in Li^6H.

TABLE VIII. - MULTIGROUP FLUX AS CALCULATED BY DISCRETE-ORDINATES METHOD

(a) In lithium hydride.

Group	Neutron flux, $\varphi_i(r)$ [neutrons/(cm^2)(sec)]/(source neutron/sec)				
	Penetration depth, r, cm				
	15	30	60	90	120
1	1.47×10^{-8}	9.16×10^{-10}	1.36×10^{-11}	3.34×10^{-13}	9.69×10^{-15}
2	6.96×10^{-8}	3.58×10^{-9}	3.70×10^{-11}	6.64×10^{-13}	1.52×10^{-14}
3	2.21×10^{-7}	9.17×10^{-9}	6.36×10^{-11}	8.36×10^{-13}	1.57
4	9.70×10^{-7}	3.12×10^{-8}	1.33×10^{-10}	1.25×10^{-12}	2.01
5	1.36×10^{-6}	3.74×10^{-8}	1.20	9.37×10^{-13}	1.38
6	2.14	5.28×10^{-8}	1.38	9.46×10^{-13}	1.32
7	4.86	1.08×10^{-7}	2.31	1.42×10^{-12}	1.89
8	4.42	9.39×10^{-8}	1.77	9.88×10^{-13}	1.26
9	2.49	5.19×10^{-8}	9.22×10^{-11}	4.94×10^{-13}	6.18×10^{-15}
10	5.48	1.13×10^{-7}	1.90×10^{-10}	9.79×10^{-13}	1.20×10^{-14}
11	9.03	1.86	2.93	1.41×10^{-12}	1.68×10^{-14}
12	6.19	1.28	1.94	8.91×10^{-13}	1.03×10^{-14}
13	6.07	1.27	1.87	8.33×10^{-13}	9.46×10^{-15}
14	1.39×10^{-5}	2.92	4.17	1.80×10^{-12}	2.01×10^{-14}
15	6.86×10^{-6}	1.44	2.03	8.66×10^{-13}	9.59×10^{-15}
16	2.02×10^{-5}	4.17	5.88	2.51×10^{-12}	2.78×10^{-14}
17	2.07	4.24	5.87	2.47	2.70
18	1.32	2.68	3.68	1.52	1.65
19	1.54	3.10	4.22	1.73	1.86
20	1.50	3.01	4.05	1.64	1.75
21	8.87×10^{-6}	1.79	2.64	1.06	1.13
22	6.92	1.38	1.84	7.36×10^{-13}	7.78×10^{-15}
23	6.79	1.35	1.79	7.16	7.55
24	3.71	7.38×10^{-8}	9.77×10^{-11}	3.89	4.10
25	2.24	4.46×10^{-8}	5.90×10^{-11}	2.35	2.47
26	2.43	4.83×10^{-8}	6.40×10^{-11}	2.54	2.68

(b) In lithium-6 hydride.

Group	Neutron flux, $\varphi_i(r)$ [neutrons/(cm^2)(sec)]/(source neutron/sec)				
	Penetration depth, r, cm				
	15	30	60	90	120
1	1.52×10^{-8}	9.77×10^{-10}	1.56×10^{-11}	4.11×10^{-13}	1.29×10^{-14}
2	7.62×10^{-8}	4.28×10^{-9}	5.22×10^{-11}	1.08×10^{-12}	2.78
3	2.40×10^{-7}	1.09×10^{-8}	9.16×10^{-11}	1.43	3.05
4	9.77×10^{-7}	3.28	1.63×10^{-10}	1.86	3.50
5	1.27×10^{-6}	3.46	1.25	1.21	2.14
6	1.91	4.58×10^{-8}	1.32	1.15	1.98
7	4.35	9.46	2.18	1.67	2.77
8	4.18	8.91	1.77	1.20	1.90
9	2.46	5.25	9.79×10^{-11}	6.20×10^{-13}	9.52×10^{-15}
10	5.40	1.15×10^{-7}	2.05×10^{-10}	1.22×10^{-12}	1.83×10^{-14}
11	8.63	1.85	3.07	1.71×10^{-12}	2.50
12	5.62	1.20	1.92	1.02×10^{-12}	1.46
13	5.23	1.11	1.73	9.07×10^{-13}	1.28
14	1.08×10^{-5}	2.25	3.46	1.79×10^{-12}	2.51
15	4.96×10^{-6}	1.02	1.56	8.03×10^{-13}	1.13
16	1.23×10^{-5}	2.50	3.86	2.01×10^{-12}	2.83
17	1.23×10^{-5}	2.46	3.74	1.91×10^{-12}	2.67
18	6.69×10^{-6}	1.33	2.00	1.01×10^{-12}	1.40
19	5.68×10^{-6}	1.12	1.67	8.42×10^{-13}	1.16
20	3.03×10^{-6}	5.95×10^{-8}	8.88×10^{-11}	4.45×10^{-13}	6.15×10^{-15}
21	9.21×10^{-7}	1.81×10^{-8}	2.69×10^{-11}	1.35×10^{-13}	1.86×10^{-15}
22	2.92×10^{-7}	5.73×10^{-9}	8.53×10^{-12}	4.29×10^{-14}	5.90×10^{-16}
23	1.15×10^{-7}	2.26×10^{-9}	3.36×10^{-12}	1.69×10^{-14}	3.32×10^{-16}
24	2.45×10^{-8}	4.82×10^{-10}	7.17×10^{-13}	3.59×10^{-15}	4.95×10^{-17}
25	6.75×10^{-9}	1.33×10^{-10}	1.98×10^{-13}	9.92×10^{-16}	1.37×10^{-17}
26	2.39×10^{-9}	4.70×10^{-11}	6.97×10^{-14}	3.52×10^{-16}	4.81×10^{-18}

REFERENCES

1. Malenfant, Richard E.: QAD: A Series of Point-Kernel General-Purpose Shielding Programs. Rep. LA-3573, Los Alamos Scientific Lab., Apr. 5, 1967.

2. Lahti, Gerald P.: QADHD Point-Kernel Radiation Shielding Computer Code to Evaluate Propellant Heating and Dose to Crew During Engine Operation. NASA TM X-1397, 1967.

3. Engle, Ward W., Jr.: A Users Manual for ANISN: A One Dimensional Discrete Ordinates Transport Code with Anisotropic Scattering. Rep. K-1693, Oak Ridge Gaseous Diffusion Plant, Mar. 30, 1967.

4. Kam, Francis B. K.; and Clark, Francis H. S.: Fission Neutron Attenuation and Gamma-Ray Buildup Factors for Lithium Hydride. Nucl. Appl., vol. 3, no. 7, July 1967, pp. 433-435.

5. Joanou, G. D.; and Dudek, J. S.: GAM-II. A B_3 Code for the Calculation of Fast-Neutron Spectra and Associated Multigroup Constants. Rep. GA-4265, General Dynamics Corp., Sept. 16, 1963.

6. Anon.: Protection Against Neutron Radiation up to 30 Million Electron Volts. Handbook 63, National Bureau of Standards, Nov. 22, 1957.

7. Casper, A. W.: Data Report and Analysis of Measurements Made in Water Behind Arrays of LiH and Li^6H. Rep. XDC-59-10-69, General Electric Co., Oct. 9, 1959.

8. West, D. L.: Data Report and Analysis of Fast Neutron Attenuation within LiH. Rep. XDC 60-1-17, General Electric Co., Dec. 30, 1959.

9. Blizard, E. P., ed.: Shielding. Vol. III, Pt. B of Reactor Handbook. Second ed., Interscience Publ. 1962, table 9-9.

10. Chapman, G. T.; and Storrs, C. L.: Effective Neutron Removal Cross Sections for Shielding. Rep. AECD-3978, Oak Ridge National Lab., Sept. 19, 1955.

11. Price, B. T.; Horton, C. C.; and Spinney, K. T.: Radiation Shielding. Pergamon Press, 1957, p. 175.

12. Goldstein, Herbert: Fundamental Aspects of Reactor Shielding. Addison-Wesley Publ. Co., Inc., 1959.

NATIONAL AERONAUTICS AND SPACE ADMINISTRATION
WASHINGTON, D. C. 20546

OFFICIAL BUSINESS

FIRST CLASS MAIL

POSTAGE AND FEES PAID
NATIONAL AERONAUTICS AND
SPACE ADMINISTRATION

"The aeronautical and space activities of the United States shall be conducted so as to contribute . . . to the expansion of human knowledge of phenomena in the atmosphere and space. The Administration shall provide for the widest practicable and appropriate dissemination of information concerning its activities and the results thereof."

—NATIONAL AERONAUTICS AND SPACE ACT OF 1958

NASA SCIENTIFIC AND TECHNICAL PUBLICATIONS

TECHNICAL REPORTS: Scientific and technical information considered important, complete, and a lasting contribution to existing knowledge.

TECHNICAL NOTES: Information less broad in scope but nevertheless of importance as a contribution to existing knowledge.

TECHNICAL MEMORANDUMS: Information receiving limited distribution because of preliminary data, security classification, or other reasons.

CONTRACTOR REPORTS: Scientific and technical information generated under a NASA contract or grant and considered an important contribution to existing knowledge.

TECHNICAL TRANSLATIONS: Information published in a foreign language considered to merit NASA distribution in English.

SPECIAL PUBLICATIONS: Information derived from or of value to NASA activities. Publications include conference proceedings, monographs, data compilations, handbooks, sourcebooks, and special bibliographies.

TECHNOLOGY UTILIZATION PUBLICATIONS: Information on technology used by NASA that may be of particular interest in commercial and other non-aerospace applications. Publications include Tech Briefs, Technology Utilization Reports and Notes, and Technology Surveys.

Details on the availability of these publications may be obtained from:

SCIENTIFIC AND TECHNICAL INFORMATION DIVISION

NATIONAL AERONAUTICS AND SPACE ADMINISTRATION

Washington, D.C. 20546